Evaluation of trabecular bone formation in a canine model surrounding a dental implant fixture immobilized with an antimicrobial peptide derived from histatin

Makihira, Seicho
Department of Oral Rehabilitation, Faculty of Dental Science, Kyushu University

Nikawa, Hiroki
Department of Oral Biology and Engineering, Graduate School of Biomedical Sciences, Hiroshima University

Shuto, Takahiro
Department of Oral Biology and Engineering, Graduate School of Biomedical Sciences, Hiroshima University

Nishimura, Masahiro
Department of Prosthetic Dentistry, Graduate School of Biomedical Sciences, Nagasaki University

他

出版情報：Journal of Materials Science : Materials in Medicine. 22 (12), pp.2765-2772, 2011-12-01. Springer US
バージョン：

Evaluation of trabecular bone formation in a canine model surrounding a dental implant fixture immobilized with an antimicrobial peptide derived from histatin

Seicho Makihira, Hiroki Nikawa, Takahiro Shuto, Masahiro Nishimura, Yuichi Mine, Koichiro Tsuji, Keishi Okamoto, Yuhiro Sakai, Masanori Sakai, Naoya Imari, Satoshi Iwata, Mika Takeda, Fumio Suehiro

Seicho Makihira, Section of Fixed Prosthodontics, Department of Oral Rehabilitation, Faculty of Dental Science, Kyushu University, Fukuoka, Japan

Hiroki Nikawa, Takahiro Shuto, Yuichi Mine, Naoya Imari, Satoshi Iwata, Department of Oral Biology and Engineering, Division of Oral Health Sciences, Graduate School of Biomedical Sciences, Hiroshima University, Hiroshima, Japan

Masahiro Nishimura, Fumio Suehiro, Department of Prosthetic Dentistry, Graduate School of Biomedical Sciences, Nagasaki University, Nagasaki, Japan

Koichiro Tsuji, Masanori Sakai, Mika Takeda, TWO CELLS Co., Ltd., Hiroshima, Japan

Keishi Okamoto, Toyo Advanced Technologies Co., Ltd. 5-3-38, Hiroshima, Japan

Yuhiro Sakai, GC Corporation, Tokyo, Japan

Corresponding author:
Seicho Makihira
Tel: +81 92 6426373
Fax: +81 92 6426374
E-mail: makihira@dent.kyushu-u.ac.jp

Key words: surface modification, antimicrobial peptide, trabecular bone, dental implant, titanium, in vivo test

Abstract JH8194 induces osteoblast differentiation, although it was originally designed to improve antifungal activity. This suggests that JH8194 is useful for implant treatment. Therefore, the aim of this study was to evaluate the osseointegration capacity of JH8194-modified titanium dental implant fixtures (JH8194-Fi). The implants were randomly implanted into the edentulous ridge of dog mandibles. Healing abutments were inserted immediately after implant placement. Three weeks later, peri-implant bone levels, the first bone-to-implant contact points, and trabecular bone formation surrounding the implants were assessed by histological and digital image analyses based on microcomputed tomography (microCT). The histological analysis revealed an enhancement of mature trabecular bone around the JH8194-Fi compared with untreated fixtures (control-Fi). Similarly, microCT combined with analysis by Zed View™ also showed increased trabecular bone formation surrounding the JH8194-Fi compared with the control-Fi (Student's *t*-test, $P < 0.05$). JH8194 may offer an alternative biological modification of titanium surfaces to enhance trabecular bone formation around dental implants, which may contribute to the transient acquirement of osseointegration and the long-term success of implant therapy.

1 Introduction

Titanium is widely used for medical devices, and in particular, pure titanium or titanium alloy are the most common materials for dental implants because of their excellent physical properties and their osseointegration potential [1]. It is widely known that the dioxide film that forms on the titanium surface increases calcium deposition and is readily reactive toward osseous proteins [1]. In addition, technological manipulations to achieve osseointegration in shorter periods and with greater strength are widely performed [1]. Numerous studies have attempted to improve the biocompatible characteristics of the titanium surface. A variety of surface modifications have been reported [2-5], including our previous work [5] in which we immobilized a cationic synthetic peptide derived from histatin, JH8194, to facilitate the differentiation of osteoblasts in vitro. The JH8194 we originally designed was synthesized to improve antifungal activity [6], and we reported successful immobilization of JH8194 to titanium surfaces through a series of previous studies [3, 7-10]. Surprisingly, we found that titanium surfaces modified with JH8194 enhanced the expression of osteoblastic differentiation markers, including Runx2 and osteopontin, in MC3T3-E1 osteoblastic cells [5], as well as suppression of biofilm formation of *Porphyromonas gingivalis* [5], a bacterium frequently recovered from peri-implantitis [11]. It is generally accepted that numerous antimicrobial peptides derived from mammalian cells have an alpha-helical structure, and the majority are cationic and amphipathic. Likewise, we previously indicated that the candidacidal activity of JH8194 was due not only to its alpha-helical propensity, but also to cationic charges [6]. The inhibitory effects of immobilized JH8194 on the titanium surface against *P. gingivalis* might be similarly attributed to the three common properties of cationic antimicrobial peptides [5, 6]. However, the mechanism of inducing osteoblast differentiation remains unclear.

In the present study, we hypothesized that JH8194-modified titanium surfaces promote the bone healing process, particularly earlier acquisition of osseointegration, in addition to the suppression of postoperative infection. Thus, in the present study, we chose to focus first on developing a bone model to evaluate the osseointegration potential of the modified implants.

To assess the osseointegration capacity of JH8194-modified titanium surfaces, we inserted dental implants into the edentulous mandible of canines and subsequently evaluated the area of new trabecular bone formation surrounding the fixture histologically from ground sections and quantitatively by the use of a three-dimensional image analysis system from the Digital Imaging and Communications in Medicine

(DICOM) data of microcomputed tomography (microCT).

2 Materials and methods

2.1 Purity of the synthetic peptide: JH8194

The JH8194 peptide was synthesized and purified to >90% at Greiner Bio-One Co., Ltd. (Tokyo, Japan) [5].

2.2 Preparation of the dental implant with JH8194

Preparation and immobilization of JH8194 on the surface of the implant fixture (GENESiO Fi IN, diameter width = 3.8 mm, length = 6.5 mm; GC, Tokyo, Japan) were carried out in accordance with the modified method described previously [5]. The implant fixtures immobilized with JH8194 (JH8194-Fi) were prepared through a series of chemical reactions. Briefly, each fixture of implants sterilized by gamma rays was immersed in 2 ml of 5% gamma-aminopropyltriethoxysilane in acetone for 15 min at room temperature and washed with 2 ml of acetone. The implant was subsequently treated with 2 ml of 5% glyoxylic acid monohydrate for 2 h and then washed with ultra-pure water. The implant surface was treated with 2 ml of 0.4% sodium borohydride ($NaBH_4$) for 24 h to reduce the imine to amine groups. The implants were then washed with ultra-pure water. The carboxyl groups on the surfaces of implant specimens were then activated with N-hydroxysuccinimide/N-ethyl-N′-(3-dimethylaminopropyl)-carbodiimide (NHS/EDC) (BiaCore AB, Uppsala, Sweden) and treated with 2 ml of 20 μM JH8194 in sodium bicarbonate buffer (pH 8.0) for 30 min at 37°C to immobilize JH8194 on the implant surface. After washing with 10 ml of phosphate-buffered saline (PBS) three times to remove the excess JH8194, the activated carboxyl groups were blocked by a 5-min treatment with 2 ml of 1 M ethanolamine-HCl (BiaCore AB). An untreated, peptide-free implant was used as a control (control-Fi).

2.3 Scanning electron microscopy observation

To examine the surface roughness and to confirm the border for two-dimensional analysis of trabecular bone formation excluding cortical bone, the surface of the implant (Fig. 1A-a) was observed under a scanning electron microscope using standard procedures (original magnification of ×30) (Fig. 1A-b) (VE-8800; Keyence, Osaka, Japan).

2.4 Surgical procedure for implantation

Four female mongrel dogs of common lineage [12] weighing 18.7 to 23.9 kg (average: 22.0 ± 2.0 kg) and 47 to 53 months of age (average: 48.8 months) were purchased from Hiroshima Animal Laboratory (Hiroshima, Japan) and used for this study. Animal selection, management, anesthesia, and surgical and analysis procedures were approved by the animal care and use committee of Hiroshima University (No. A09-30, Hiroshima, Japan). The in vivo experiments using the dog model were performed in accordance with the procedures allowed by the committee.

The implantation involved two surgical procedures (Fig. 1C). First, the second and third premolars on the bilateral sides were extracted to prepare the alveolar bone without teeth two months before the implant operation (Fig. 1C-a). The 16 sites without teeth were totally prepared. After confirming bone healing of tooth extraction sites, either a control-Fi (n = 4) or a JH8194-Fi (n = 4) was randomly placed into the edentulous ridge of each dog mandible (Fig. 1C-b and c). Seven implants were inserted under torque between 10 N·cm ≤ initial fixation ≤ 40 N·cm according to a general procedure that may be considered suitable to acquire primary stability. Because the torque of one implant in four control fixtures was >60 N·cm, it was excluded from the experiment. The other eight implants were placed into the edentulous ridge of each dog mandible for another independent project (not shown). The platforms of all implants were aligned with the alveolar ridge according to the manufacturer's instructions. The healing abutment recommended in the instructions was placed on the platform after fixture implantation (ABUTMENT IN, diameter width = 5.0 mm, collar height = 4.0 mm; GC) (Fig. 1C-c), and gingival tissues were sutured with degradable surgical sutures (Vicryl; Johnson & Johnson, Tokyo, Japan).

2.5 Computed tomographic analysis

Three weeks after fixture implantation [13, 14], dog mandibles were harvested, dissected without decalcification, fixed in 10% formalin solution for 48 h, and dehydrated through a graded ethanol series for one week.

DICOM data were obtained by the use of microCT (Toscaner; Toshiba, Tokyo, Japan) for each specimen oriented with the vertical axis perpendicular to the ground. The scans by microCT were carried out under the conditions; X-ray tube voltage of 100.0 kV, tube current of 62 μA, slice thickness of 0.05 mm, slice pitch of 0.05 mm and view numbers of 400. DICOM data obtained from the microCT examination were analyzed by Zed View™ (ZV) software (Lexy, Tokyo, Japan) to evaluate the area of trabecular bone within the defined region surrounding each implant fixture.

A schematic model of the implant is shown in Figure 1B. The center line (Center Line) of the mediodistal direction on the fixture platform was defined as equidistant from both edges of the lingual and buccal cortical bone (Fig. 1B). Two fiduciaries (points A and B) for analysis by ZV were decided from the nadir at the bottom (point A) and the central point at the top (point B) of the sagittal plane, respectively (Fig. 1B). The longitudinal line (Longitudinal Line) linked point A with point B. The evaluation of the distance between the medial (distal) line and the longitudinal line was denoted as the evaluation width (Evaluation Width = 3, 4, or 5 mm). The X-axis in the evaluation area (Evaluation Area) was parallel to the Center Line, while the Y-axis in the Evaluation Area was parallel to the Longitudinal Line. The top of the X-axis was positioned on the indicated line corresponding to the white arrowhead of Figure 1A-b (Fig. 1B) to stay off the cortical bone. The EA was equally divided into two areas: the lower (EA (lower)) and upper (EA (upper)) halves. The area of trabecular bone in the Evaluation Area was automatically calculated when the Evaluation Area, ranges of mask, and intensity were defined with ZV. To eliminate the implant fixture from the images, the constant ranges of masks and intensity of ZV in this study were $40 \leq \text{mask} \leq 200$ and $30 \leq \text{intensity} \leq 300$, respectively, for all analyses. The implant could not be masked under these optimal conditions using ZV.

2.6 Histological analysis

After microCT examination of each specimen, the dehydrated specimens were embedded in methyl

methacrylate for histological analysis. Mesiodistal and longitudinal sections were ground to a thickness of 100 to 120 μm and stained with Villanueva-Goldner (VG) to evaluate new bone formation and to distinguish mature and immature bone [15] (Kureha Special Laboratory, Tokyo, Japan). The red regions in the sections stained with VG indicate immature trabecular bone, and the green regions indicate mature trabecular bone. A photographic image of each section was taken with a digital camera attached to a stereomicroscope (original magnification of ×12.5).

2.7 Statistical analysis

Data were analyzed by a one-way analysis of variance (ANOVA) and Dunnett's multiple range test, or Student's *t*-test (t-test).

3 Results

The postoperative states of the gingival tissues surrounding the healing abutment were carefully examined weekly. There were no remarkable inflammatory symptoms in the oral mucosa surrounding the dental implants of either the control-Fi or JH8194-Fi groups. In addition, there were no remarkable changes in the body weights of the dogs throughout the study (not shown).

3.1 Alteration of mature and immature trabecular bone surrounding the control-Fi and JH8194-Fi implants

Representative photographs of the histological sections stained by VG are shown in Figure 2. In general, the areas of positively stained mature trabecular bone (green portions) were larger surrounding the JH8194-Fi implants than those surrounding the control-Fi implants (Fig. 2, white arrowheads). In contrast, the red areas of immature trabecular bone were smaller than those of the control-Fi implants (Fig. 2, blue arrowheads).

3.2 Quantitative comparison of the trabecular bone area in contact with control-Fi and JH8194-Fi implants

Representative images in the two-dimensional analysis combined with microCT and ZV are shown in Figure 3A. With the ZV software, the trabecular bone surrounding the implant was masked as green, enabling a quantitative comparison of the trabecular bone area in contact with the implants in the samples. When EW = 3, the area of trabecular bone around the JH8194-Fi was significantly increased compared with that around the control-Fi (t-test, $P < 0.05$) (Fig. 3B). At EW = 4 and 5, the mean values of the area of trabecular bone were greater with the JH8194-Fi compared with control-Fi; however, there were no significant differences in the area of trabecular bone at the EA between the control-Fi and JH8194-Fi (t-test, $P > 0.05$) (Fig. 3B).

Similar to the case of the EA, the trabecular bone in the EA (upper) and EA (lower) surrounding the JH8194-Fi was greater than that in the EA (upper) and EA (lower) surrounding the control-Fi (Fig. 3C). As for the EA (lower), trabecular bone that formed around JH8194-Fi was significantly greater than that of control-Fi (ANOVA, $P < 0.05$). On the other hand, there was no significant difference in the trabecular bone formation between the control-Fi and the JH8194-Fi at EA (upper) (ANOVA, $P > 0.05$) (Fig. 3C).

4 Discussion

At present, many studies have carried out animal experiments to apply in vitro titanium surface modifications [16-19] to in vivo conditions, including the implantation of titanium implants modified with diamond-like carbon coatings [16], RGD peptide [20], and recombinant bone morphogenetic protein (BMP)-2 [21, 22], as well as prototypes of dental implant fixtures with a variety of surface modifications [16, 20-22]. Such prototypes have been implanted into the jaw bone [22-25], limb [26], or tibia [27, 28] of experimental animals including rats [27, 28], rabbits [26], dogs [22-25], and sheep [29]. Similarly, numerous types of radiographic and histological analyses of new bone formation surrounding implants after the operation were carried out [16, 21-26, 28-31]. Collectively, these reports suggest that a larger laboratory animal model, such as a dog, is potentially more representative of the human in vivo environment compared with smaller animal models because the implant can be entirely inserted into the jaw [16, 21-26, 28-31]. Moreover, histological and microCT digital image analyses of the trabecular bone

that is closely associated with osseointegration of the implant can provide a holistic quantitative and qualitative evaluation of the osteogenic potential of the surface-modified titanium. Therefore, in the present study, we employed a dog model and attempted to investigate whether a JH8194-immobilized titanium implant can accelerate or increase mature trabecular bone around the implanted fixture using ZV with DICOM data from microCT; in addition, we performed a conventional histological analysis [15]. In microCT analysis, metal artifacts could not be avoided. However, we considered that the metal artifacts in the comparative analysis of the present study were negligible, since the conditions of the small noises around both of control and prototype implants were theoretically equal.

Histatin 5 is the most potent member of the antifungal peptide family and renders most pathogenic *Candida* species nonviable in vitro at physiological concentrations [32]. In a previous study, the results of a biofilm assay using *P. gingivalis*, a common bacterium involved in peri-implantitis [11], demonstrated that JH8194 immobilized on the titanium disc surface by the same immobilization method used in the present study inhibited biofilm formation of *P. gingivalis* as predicted [5]. However, a surprising finding was that the JH8194 immobilized on the titanium surface accelerated osteoblast differentiation [5]. Research including animal studies could potentially validate these findings. However, it was difficult to plan the in vivo experiment model to simultaneously confirm two potentials of JH8194-immobilized titanium (osseointegration and protection from early bacterial infection) because intentionally simulating initial infection at surgery around the Fi may influence normal osseointegration in the oral cavity of the dog. In addition, anterior and posterior antibiotic loads in surgery are normally required in animal experiments to avoid postoperative infection [21, 22]. Therefore, we decided that initial experiments would evaluate the potential osseointegration of JH8194-Fi in the present study. In the future, further investigations will clarify the possible function of JH8194 in providing protection from early bacterial infections suggested by our in vitro data [5].

Thus, the main purpose of this study was to clarify whether the prototype implant with JH8194 enhanced osseointegration. Surprisingly, the in vivo data obtained from the dog model indicated that JH8194-Fi increased the mature trabecular bone formation surrounding the implant compared with control-Fi. In addition, the trabecular bone composed of the immature trabecular bone and mature trabecular bone that were stained with VG were not completely equal. The results obtained from both digital data and histological analysis strongly suggest that JH8194-Fi enhanced osseointegration compared with the

control-Fi. The significant enhancement of trabecular bone formation by JH8194 was observed not at EW = 4 or 5, but at EW = 3 (Fig. 3B), which suggests that this enhancement was directly involved in JH8194. Based on a previous in vitro study [5] and the present in vivo data, the in vitro enhancement of osteoblast differentiation by titanium discs immobilized with JH8194 may reflect the in vivo increase of mature trabecular bone in contact with implanted JH8194-Fi.

In vitro experiments have shown that collagen and RGD peptides immobilized onto titanium enhanced the adhesion of osteoblast cells in as early as 1 day [3, 33]. Collagen I coatings of dental screw implants enhanced peri-implant bone formation in 1 month [21, 34]. BMPs are generally known to increase bone formation, and BMPs released from atelopeptide type I collagen (carrier) have been reported to stimulate a bone response in peri-implants [35]. However, BMP immobilized on titanium did not show an increase in peri-implant bone formation after 1 and 3 months in vivo [34]. These reports suggest that the conformation and/or activity of the molecule after the immobilization process are very important for the function of the immobilized protein [3, 21, 33-35]. The present study suggests that our immobilization method had minimum effects on the conformation and/or activity of the JH8194 peptide. Based on our previous report in which we found that osteoprotegerin immobilized on a titanium surface was slowly released from the titanium surface [3], we speculate that functional JH8194 may remain on the surface of the implant without degradation or that the immobilized JH8194 may be slowly released from the surface of the implant.

It was important to examine whether or not mechanical forces simulating insertion of dental implants cause abrasion of JH8194 binding to the titanium surface. Although the proper in vitro methodology to test abrasion is not established to test this procedure, a surgical technique has been reported to avoid abrasion of the material coating of the titanium surface during insertion [21]. In the present study, however, we chose a standard surgical procedure without avoiding a risk of abrasion of the material coating because the final goal of this project was to develop an alternative fixture possessing a surface modified with JH8194 that can be implanted in accordance with routine surgical procedures widely used at present [31]. In addition, JH8194 was immobilized through covalent bonding to the titanium surface; hence, it could be predicted that the risk of detachment of the peptides by mechanical stress would be minimal. Indeed, the results suggest that JH8194 was successfully immobilized to the surface of the titanium implant, was not largely affected by abrasion following mechanical insertion into the mandible, and consequently led to the increase of mature trabecular bone formation around the implant. We initially speculated that the peptides

immobilized to the lower portion of the fixtures were more susceptible to abrasion; however, the present in vivo study using the standard surgical procedure suggests that this risk was minimal because the increased tendency of the trabecular bone in the EA (lower) by JH8194-Fi was similar to that of the EA (upper) according to ZV analysis (Fig. 3C).

The present study using a canine model, an analysis method of ground sections and microCT, and the widely accepted standard surgical procedure for implantation validated the hypothesis that a prototype of JH8194-Fi fabricated according to our immobilization method could induce osseointegration. Specifically, JH8194-Fi significantly enhanced trabecular bone formation, leading to accelerated osseointegration. Further investigations will be performed to clarify whether JH8194-modified implant fixtures can provide protection from early bacteria colonization using a modified canine model simulating early infection.

5 Conclusion

JH8194, an antimicrobial peptide derived from histatin, immobilized on a titanium surface enhanced mature trabecular bone formation surrounding the implant three weeks following implantation. Thus, JH8194 is a potential candidate as a biological surface modifier of dental implants to enhance osseointegration, potentially leading to the long-term stability of dental implants and hopefully an increased rate of implant treatment success.

Acknowledgments This study was performed with the cooperation of the Regional Innovation Creation Research and Development Business Program of the Japan Ministry of Economy, Trade and Industry in Japan (2008-2009). The authors thank Mr. K. Mamada, Mr. L. Takanohashi, Mr. H. Yoshihara (GC Corporation), and Mr. S. Okazaki (Hiroshima University) for their kind technical support in surgery and in the microCT examinations.

References

1. Avila G, Misch K, Galindo-Moreno P, Wang HL. Implant surface treatment using biomimetic agents. Implant Dent. 2009;18:17-26.

2. Degasne I, Basle MF, Demais V, Hure G, Lesourd M, Grolleau B, et al. Effects of roughness, fibronectin and vitronectin on attachment, spreading, and proliferation of human osteoblast-like cells (Saos-2) on titanium surfaces. Calcif Tissue Int. 1999;64:499-507.
3. Schuler M, Owen GR, Hamilton DW, de Wild M, Textor M, Brunette DM, et al. Biomimetic modification of titanium dental implant model surfaces using the RGDSP-peptide sequence: a cell morphology study. Biomaterials. 2006;27:4003-15.
4. Makihira S, Mine Y, Nikawa H, Shuto T, Kosaka E, Sugiyama M, et al. Immobilized-OPG-Fc on a titanium surface inhibits RANKL-dependent osteoclast differentiation in vitro. J Mater Sci Mater Med. 2010;21:647-53.
5. Makihira S, Shuto T, Nikawa H, Okamoto K, Mine Y, Takamoto Y, et al. Titanium immobilized with an antimicrobial peptide derived from histatin accelerates the differentiation of osteoblastic cell line, MC3T3-E1. Int J Mol Sci. 2010;11:1458-70.
6. Nikawa H, Fukushima H, Makihira S, Hamada T, Samaranayake LP. Fungicidal effect of three new synthetic cationic peptides against Candida albicans. Oral Diseases. 2004;10:221-8.
7. Satou N, Satou J, Shintani H, Okuda K. Adherence of streptococci to surface-modified glass. J Gen Microbiol. 1988;134:1299-305.
8. Nikawa H, Sadamori S, Hamada T, Satou N, Okuda K. Non-specific adherence of Candida species to surface-modified glass. J Med Vet Mycol. 1989;27:269-71.
9. Nikawa H, Sadamori S, Hamada T, Okuda K. Factors involved in the adherence of Candida albicans and Candida tropicalis to protein-adsorbed surfaces. An in vitro study using immobilized protein. Mycopathologia. 1992;118:139-45.
10. Martin HJ, Schulz KH, Bumgardner JD, Walters KB. XPS study on the use of 3-aminopropyltriethoxysilane to bond chitosan to a titanium surface. Langmuir. 2007;23:6645-51.
11. Quirynen M, De Soete M, van Steenberghe D. Infectious risks for oral implants: a review of the literature. Clin Oral Implants Res. 2002;13:1-19.
12. Hagihara A, Sugiyama A, Hashimoto K. Effects of antiarrhythmic drugs on the monophasic action potential of the canine isolated, blood-perfused ventricular septum preparation. Heart Vessels. 1998;13:181-8.
13. Schliephake H, Scharnweber D, Dard M, RoBler S, Sewing A, Huttmann C. Biological performance of biomimetic calcium phosphate coating of titanium implants in the dog mandible. J Biomed Mater Res 2003; 64A: 225-234.
14. Ume W, Qahash M, Polimeni G, Susin C, Shanaman RH, Rohrer MD, Wozney JM, Hall J. Alveolar ridge augmentation using implants coated with recombinant human bone morphogenic protein-2:

histologic observations. J Clin Periodontol 2008; 35: 1001-1010.

15. Jang BJ, Byeon YE, Lim JH, Ryu HH, Kim WH, Koyama Y, et al. Implantation of canine umbilical cord blood-derived mesenchymal stem cells mixed with beta-tricalcium phosphate enhances osteogenesis in bone defect model dogs. J Vet Sci. 2008;9:387-93.
16. Allen M, Myer B, Rushton N. In vitro and in vivo investigations into the biocompatibility of diamond-like carbon (DLC) coatings for orthopedic applications. J Biomed Mater Res. 2001;58:319-28.
17. Puleo DA, Kissling RA, Sheu MS. A technique to immobilize bioactive proteins, including bone morphogenetic protein-4 (BMP-4), on titanium alloy. Biomaterials. 2002;23:2079-87.
18. Zreiqat H, Akin FA, Howlett CR, Markovic B, Haynes D, Lateef S, et al. Differentiation of human bone-derived cells grown on GRGDSP-peptide bound titanium surfaces. J Biomed Mater Res. 2003;64:105-13.
19. Chai F, Mathis N, Blanchemain N, Meunier C, Hildebrand HF. Osteoblast interaction with DLC-coated Si substrates. Acta Biomater. 2008;4:1369-81.
20. Rammelt S, Illert T, Bierbaum S, Scharnweber D, Zwipp H, Schneiders W. Coating of titanium implants with collagen, RGD peptide and chondroitin sulfate. Biomaterials. 2006;27:5561-71.
21. Schliephake H, Aref A, Scharnweber D, Bierbaum S, Roessler S, Sewing A. Effect of immobilized bone morphogenic protein 2 coating of titanium implants on peri-implant bone formation. Clin Oral Implants Res. 2005;16:563-9.
22. Lee J, Decker JF, Polimeni G, Cortella CA, Rohrer MD, Wozney JM, et al. Evaluation of implants coated with rhBMP-2 using two different coating strategies: a critical-size supraalveolar peri-implant defect study in dogs. J Clin Periodontol. 2010;37:582-90.
23. Carmagnola D, Araujo M, Berglundh T, Albrektsson T, Lindhe J. Bone tissue reaction around implants placed in a compromised jaw. J Clin Periodontol. 1999;26:629-35.
24. Gotfredsen K, Berglundh T, Lindhe J. Bone reactions adjacent to titanium implants with different surface characteristics subjected to static load. A study in the dog (II). Clin Oral Implants Res. 2001;12:196-201.
25. Calvo-Guirado JL, Ortiz-Ruiz AJ, Negri B, Lopez-Mari L, Rodriguez-Barba C, Schlottig F. Histological and histomorphometric evaluation of immediate implant placement on a dog model with a new implant surface treatment. Clin Oral Implants Res. 2010;21:308-15.
26. Suzuki M, Calasans-Maia MD, Marin C, Granato R, Gil JN, Granjeiro JM, et al. Effect of surface modifications on early bone healing around plateau root form implants: an experimental study in rabbits. J Oral Maxillofac Surg. 2010;68:1631-8.

27. Kajiwara H, Yamaza T, Yoshinari M, Goto T, Iyama S, Atsuta I, et al. The bisphosphonate pamidronate on the surface of titanium stimulates bone formation around tibial implants in rats. Biomaterials. 2005;26:581-7.
28. Maekawa K, Shimono K, Oshima M, Yoshida Y, Van Meerbeek B, Suzuki K, et al. Polyphosphoric acid treatment promotes bone regeneration around titanium implants. J Oral Rehabil. 2009;36:362-7.
29. Gutwald R, Haberstroh J, Stricker A, Ruther E, Otto F, Xavier SP, et al. Influence of rhBMP-2 on bone formation and osseointegration in different implant systems after sinus-floor elevation. An in vivo study on sheep. J Craniomaxillofac Surg. 2010;38:571-9.
30. Lee BH, Kim JK, Kim YD, Choi K, Lee KH. In vivo behavior and mechanical stability of surface-modified titanium implants by plasma spray coating and chemical treatments. J Biomed Mater Res. 2004;69:279-85.
31. Coelho PG, Marin C, Granato R, Bonfante EA, Lima CP, Suzuki M. Surface treatment at the cervical region and its effect on bone maintenance after immediate implantation: an experimental study in dogs. Oral Surg Oral Med Oral Pathol Oral Radiol Endod. 2010;110:182-7.
32. Raj PA, Edgerton M, Levine MJ. Salivary histatin 5: dependence of sequence, chain length, and helical conformation for candidacidal activity. J Biol Chem. 1990;265:3898-905.
33. Muller R, Abke J, Schnell E, Scharnweber D, Kujat R, Englert C, et al. Influence of surface pretreatment of titanium- and cobalt-based biomaterials on covalent immobilization of fibrillar collagen. Biomaterials. 2006;27:4059-68.
34. Mandelin J, Li TF, Liljestrom M, Kroon ME, Hanemaaijer R, Santavirta S, et al. Imbalance of RANKL/RANK/OPG system in interface tissue in loosening of total hip replacement. J Bone Joint Surg Br. 2003;85:1196-201.
35. Schneeweis LA, Willard D, Milla ME. Functional dissection of osteoprotegerin and its interaction with receptor activator of NF-kappaB ligand. J Biol Chem. 2005;280:41155-64.

Figure captions

Fig. 1. A representative photograph of the implant used in the present study (A-a). The edge of the implant for the two-dimensional analysis was observed by scanning electron microscopy (A-b). A schematic of the implant fixture explaining the defined points (points A and B), lines (Center Line and Longitudinal Line), and axes (X-axis and Y-axis) for evaluating the trabecular bone area in the Evaluation Area, Evaluation Area (lower), and Evaluation Area (upper) using ZV software (B). The Evaluation Width (3, 4, or 5 mm)

was changed for each analysis. The fixture was implanted into the canine edentulous mandible (C-b), which was prepared by the extraction of teeth according to a standard procedure (C-a) described in the Materials and Methods (C-c).

Fig. 2. Representative photographs at ×12.5 original magnification obtained from ground sections stained with VG. The staining demonstrated the area of trabecular bone and distinguished mature (white arrowhead) and immature (blue arrowhead) bone around the inserted implants within the edentulous ridge.

Fig. 3. Representative images obtained by microCT and ZV. The green portions illustrated in the Evaluation Area were automatically recognized as the trabecular bone area by the ZV software under optimal conditions. The white area indicates the implant fixture in the longitudinal and mesiodistal directions under the same conditions. Representative images of the control-Fi and JH8194-Fi at three weeks are shown (A). The mean occupied area of the trabecular bone (%) in the Evaluation Area (lower + upper) (3, 4, and 5 mm) was calculated by the ZV software (B). The values are expressed as the mean ± SD. The asterisks indicate a statistically significant difference compared with the other test group (t-test; $*P < 0.05$). The mean area of the trabecular bone (%) in the EA (upper or lower) (3 mm) is shown (± SD) (C). The asterisks indicate a statistically significant difference for all samples (ANOVA; $*P < 0.05$).

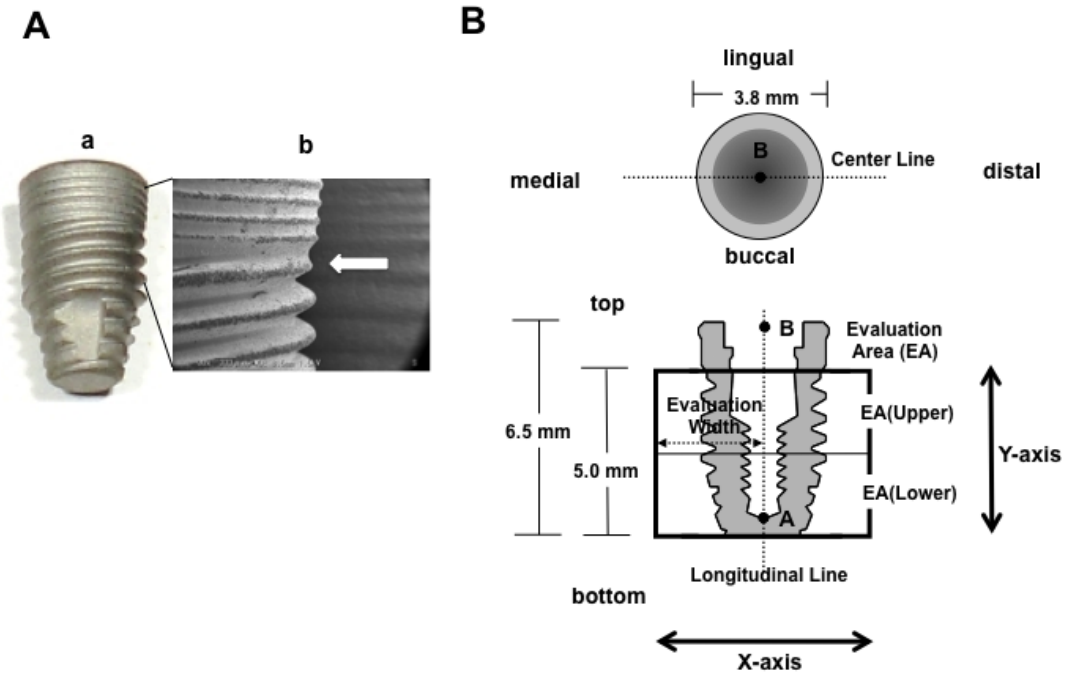

Fig. 1. S. Makihira et. al.

C

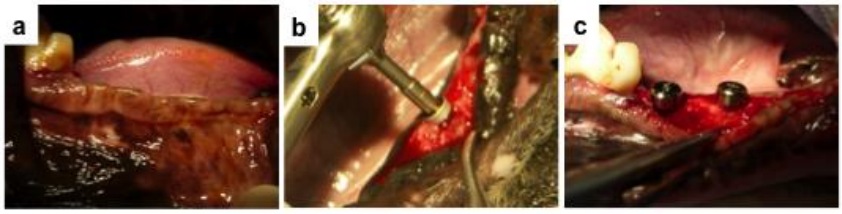

Fig. 1. S. Makihira et. al.

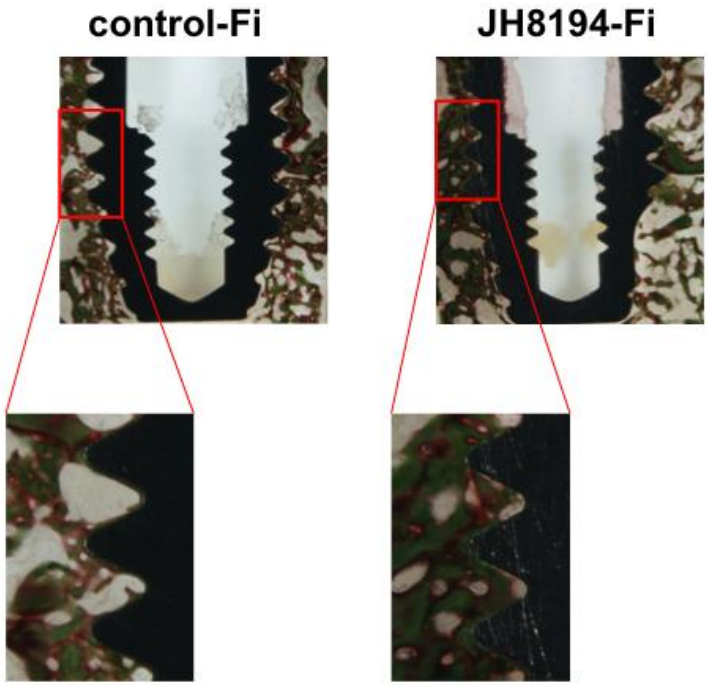

Fig. 2. S. Makihira et. al.

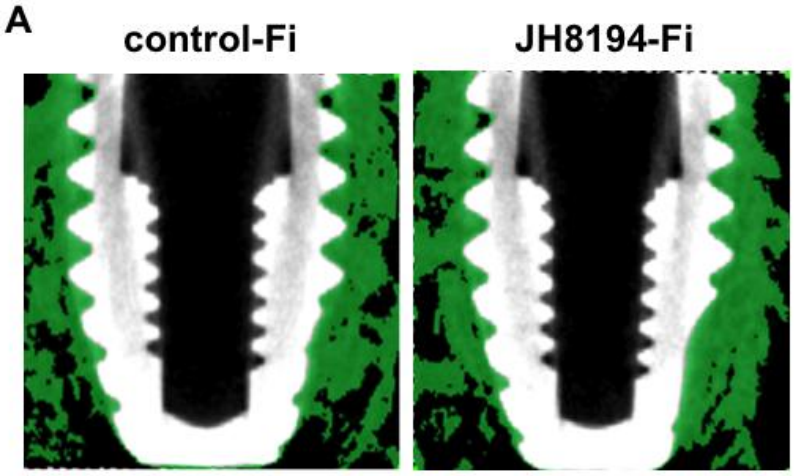

Fig. 3. S. Makihira et. al.

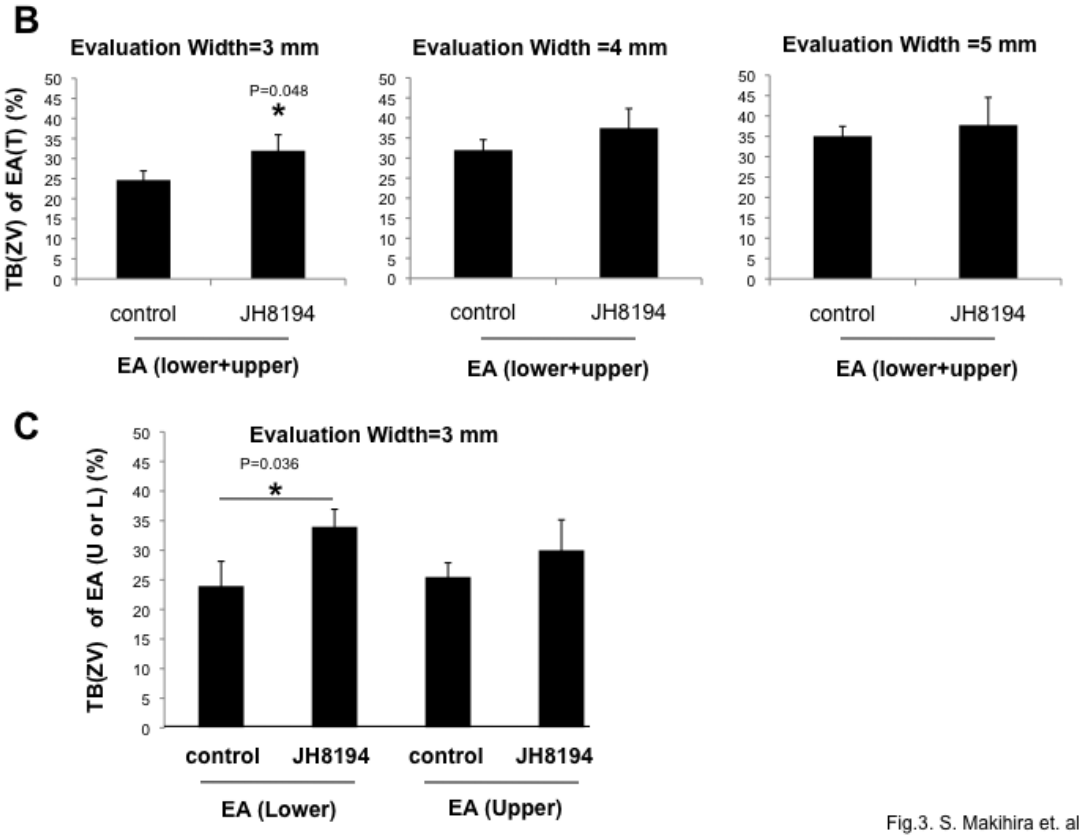

Fig.3. S. Makihira et. al.